

## Distinct Metal Environment in Fe-Substituted Manganese Superoxide Dismutase Provides a Structural Basis of Metal Specificity

Ross A. Edward,<sup>1a</sup> Mei M. Whittaker,<sup>1b</sup> James W. Whittaker,<sup>1b</sup> Geoffrey B. Jameson,<sup>\*,1a</sup> and Edward N. Baker<sup>\*,1c</sup>

Center for Structural Biology, Institutes of Fundamental Sciences and Molecular Biosciences Massey University, Palmerston North, New Zealand  
Department of Biochemistry and Molecular Biology Oregon Graduate Institute, P.O. Box 91000 Portland, Oregon 97291-1000

Received March 31, 1998

The structures of several native iron<sup>2</sup> and manganese<sup>2c,3</sup> superoxide dismutases (FeSOD and MnSOD) from a variety of species reveal a remarkable conservation of structure for the metal-binding site of these enzymes, which are of physiological importance to aerobes.<sup>4</sup> The active sites are extremely similar in all MnSOD and FeSOD structures and undergo only minor changes in geometry when the metal ion is oxidized or reduced,<sup>2c,3b</sup> suggesting that the geometry is imposed by the protein on the metal. Despite the high degree of structural homology between Fe and MnSODs, replacement of the native metal (Fe or Mn) by the other results in nearly complete loss of activity for many<sup>5</sup> (but not all<sup>5b–e</sup>) Fe and MnSODs. Here we report the first structure of an Fe or MnSOD containing the “wrong” metal ion in the active site. Whereas native MnSOD and FeSOD with less than 50% sequence identity have identical active-site structures, iron-substituted MnSOD (Fe–MnSOD) and MnSOD with 100% sequence identity show marked differences in their active sites.

Fe–MnSOD was prepared and purified as previously described,<sup>6</sup> except that the medium was supplemented with iron salts. Quantitative uptake of iron was confirmed by atomic absorption spectrometry. Crystals were grown at pH 8.5 under conditions similar to those for MnSOD,<sup>3d</sup> except that azide was excluded and 0.2 M MgCl<sub>2</sub> was required. Salient details of data collection and refinement are summarized below.<sup>7</sup>

The stereochemistries of the metal sites of native Mn and FeSODs are extremely similar, as illustrated in Figure 1 for the

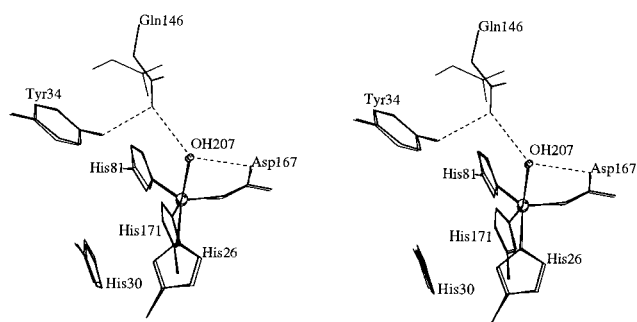


**Figure 1.** Stereodiagram of the metal environment of native FeSOD<sup>2c</sup> (thin lines) and MnSOD<sup>3d</sup> (thick lines) from *E. coli*, illustrating the very similar stereochemistries. Respectively, the axial angles are 174° and 175°, and the equatorial angles range from 113° to 127° and 111° to 129°.

Fe<sup>2c</sup> and MnSODs<sup>3d</sup> from *E. coli*. These two proteins have 45% sequence identity and both enforce trigonal-bipyramidal geometry on their native metal ions. Comparison of the two structures shows that (i) bond angles have an RMS difference of only 2.7° (maximum difference 5°); (ii) bond distances have an RMS difference of 0.15 Å (maximum difference 0.20 Å, mostly attributable to redox heterogeneity Mn(II)/Mn(III) in the MnSOD crystal); (iii) ligand orientations differ by at most 12°; and (iv) positions of residues that form a hydrogen-bonded network around the axial solvent are very similar.

In contrast the active site structures for Fe–MnSOD and native MnSOD (shown in Figure 2) are remarkably different, although the protein framework is unchanged by metal substitution.<sup>7a</sup> Relative to the trigonal-bipyramidal arrangement of ligands in MnSOD, these ligands surround the Fe *at both sites* in Fe–MnSOD in a distorted square-pyramidal geometry, leading to an increase in the N<sup>81</sup>–Fe–N<sup>171</sup> bond angle of ~20° (to 148°) with a concomitant decrease in the N<sup>171</sup>–Fe–O<sup>167</sup> bond angle by ~15°. Comparing Fe–MnSOD with MnSOD (FeSOD in parentheses), the RMS difference in bond angles is 8.1° (9.0°). The axial direction changes from OW<sup>207</sup>–Mn–N<sup>26</sup> to O<sup>167</sup>–Fe. Substantial reorientations occur for side chains in both the inner and outer coordination spheres, although the basic connectivity of the hydrogen bonding network is preserved.

(7) (a) X-ray diffraction data were collected by an RAxis IIC/RU200 system on a very thin needle-shaped crystal (~0.015 × 0.030 × 1.0 mm) to a resolution of 2.2 Å at 110 K. Crystallographic methods were as previously described,<sup>3d</sup> except X-plor/CNS<sup>7b</sup> was used to remove phasing bias from the MnSOD structure. Crystal data: orthorhombic C222<sub>1</sub>; *a* = 46.19, *b* = 89.04, *c* = 206.67 Å, *Z* = 2 (one dimer); 19 120 unique data; completeness = 93.2% (outermost shell, 82.6%); *R*<sub>merge</sub> = 0.090 (outermost shell, 0.266); current *R* = 0.205 (*R*<sub>free</sub> = 0.234 for 1563 reflections set aside from refinement and Fourier calculations); RMS (bond distances) = 0.006 Å; RMS (bond angles) = 1.3°; 90.6% of residues in the most-favored regions of a Ramachandran plot;<sup>7c</sup> 205 × 2 residues, 3256 protein atoms, 2 Fe(III), 3 solvent-derived ligands, 228 water molecules. Considerable confidence can be placed in comparisons between the structures of MnSOD and Fe–MnSOD, since the former is the average of four crystallographically independent chains (where the only significant differences are found at intermolecular contacts between dimers) and the latter is the average of two such chains (where differences are concentrated at the metal sites and intermolecular contacts between dimers). Global alignment of Fe–MnSOD and MnSOD structures yields an RMS difference of only 0.27 Å for ~800/820 main-chain atoms, a value similar to the variations found between the two crystallographically independent chains comprising Fe–MnSOD and among the four such chains of MnSOD.<sup>3d</sup> With one exception,<sup>7d</sup> the entire structure is extremely well ordered (*B*<sub>average</sub> (main chain atoms) = 12 Å<sup>2</sup>). (b) Brünger, A. T.; Adams, P. D.; Clore, G. M.; Gros, P.; Grosse-Kunstleve, R. W.; Jiang, J.-S.; Kuszewski, J.; Nilges, M.; Pannu, N. S.; Read, R. J.; Rice, L. M.; Simonson, T.; Warren, G. L. *Acta Crystallogr. D* 1998, 54, in press. (c) Laskowski, R. A.; MacArthur, M. W.; Moss, D. S.; Thornton, J. M. *J. Appl. Crystallogr.* 1993, 26, 283–291. (d) In chain B, the high *B* value for OW<sup>208</sup> indicates loose attachment (or incomplete occupancy) at the sixth coordination site; in chain A, Tyr<sup>34</sup> appears to be disordered. Annealed omit maps for the iron sites are provided in Supporting Information to show the presence (chain B) and absence (chain A) of a sixth ligand at the iron sites.

\* To whom correspondence should be addressed at (a) Centre for Structural Biology, Institute of Fundamental Sciences, Massey University, Palmerston North, New Zealand, Phone (64) (6) 350-4431, FAX (64) (6) 350-5682, E-mail G.B.Jameson@massey.ac.nz; (b) School of Biological Sciences, University of Auckland, P.O. Box 92-019, Auckland, New Zealand. Phone (64) (9) 373-7599 x4415, FAX (64) (9) 373-7619, E-mail: Ted.Baker@auckland.ac.nz.

(1) (a) Institute of Fundamental Sciences. (b) Oregon Graduate Institute. (c) Institute of Molecular Biosciences. Current address: University of Auckland.

(2) (a) Stoddard, B. L.; Howell, P. L.; Ringe, D.; Petsko, G. A. *Biochemistry* 1990, 29, 8885–8893. (b) Cooper, J. B.; McIntyre, K.; Badasso, M. O.; Wood, S. P.; Zhang, Y.; Garbe, T. R.; Young, D. J. *Mol. Biol.* 1995, 246, 531–544. (c) Lah, M. S.; Dixon, M. M.; Patridge, K. A.; Stallings, W. C.; Fee, J. A.; Ludwig, M. L. *Biochemistry* 1995, 34, 1646–1660. (d) Lim, J.-H.; Yu, Y. G.; Han, Y. S.; Cho, S.; Ahn, B.-Y.; Cho, Y. *J. Mol. Biol.* 1997, 270, 259–274.

(3) (a) Parker, M. W.; Blake, C. C. F. *J. Mol. Biol.* 1988, 199, 649–661. (b) Ludwig, M. A.; Metzger, A. L.; Patridge, K. A.; Stallings, W. C. *J. Mol. Biol.* 1991, 219, 335–358. (c) Borgstahl, G. E. O.; Parge, H. E.; Hickey, M. J.; Beyer, Jr., W. F.; Hallewell, R. A.; Tainer, J. A. *Cell* 1992, 71, 107–118. (d) Edwards, R. A.; Baker, H. M.; Whittaker, M. M.; Whittaker, J. W.; Jameson, G. B.; Baker, E. N. *J. Biol. Inorg. Chem.* 1998, 3, 161–171.

(4) (a) McCord, J. M.; Fridovich, I. *Free Radical Biol. Med.* 1988, 5, 363–369. (b) Fridovich, I. *J. Biol. Chem.* 1977, 272, 18515–18517.

(5) (a) Weatherburn, D. C. *Persp. Bioinorg. Chem.* 1996, 3, 1–113. (b) Schmidt, M.; Meier, B.; Parak, F. *J. Biol. Inorg. Chem.* 1996, 1, 532–541. (c) Martin, M. E.; Byers, B. R.; Olson, M. O. J.; Salin, M. L.; Arceneaux, J. E. L.; Tolbert, C. *J. Biol. Chem.* 1986, 261, 9361–9367. (d) Pennington, C. D.; Gregory, E. M. *J. Bacteriol.* 1986, 166, 528–532. (e) Meier, B.; Barra, D.; Bossa, F.; Calabrese, L.; Rotilio, G. *Biol. Chem.* 1982, 257, 13977–13980.

(6) Whittaker, J. W.; Whittaker, M. M. *J. Am. Chem. Soc.* 1991, 113, 5528–5540.

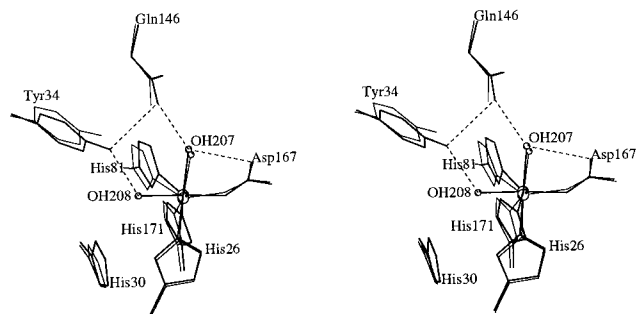


**Figure 2.** Stereodiagram of the metal environment for chain B of Fe-substituted MnSOD (thick lines) and native MnSOD<sup>3d</sup> (thin lines) from *E. coli*, illustrating the significantly different stereochemistries. The metal environment of Fe in chain A is identical to that for chain B, except for the absence of OW<sup>208</sup> and orientation of Tyr<sup>34</sup>. Metal–ligand bond distances (in Å) and angles (in deg) are highlighted in boldface when differences between Fe–MnSOD (respectively, chain A and B) and MnSOD (in parentheses) exceed 0.1 Å and 15°. Histidine ligands, residues 26, 81, 171, bind to the metal through atom NE2, Asp167 binds through atom OD2, and solvent-derived ligands are denoted OW. Fe–N<sup>26</sup> 2.15, 2.15 (2.19); Fe–OW<sup>207</sup> 2.20, 2.30 (2.24); **Fe–N<sup>81</sup> 2.08, 2.13 (2.25)**; **Fe–N<sup>171</sup> 2.28, 2.30 (2.19)**; Fe–O<sup>167</sup> 2.07, 1.98 (2.05); N<sup>26</sup>–Fe–OW<sup>207</sup> 173, 179 (175); N<sup>26</sup>–Fe–N<sup>81</sup> 89, 94 (92); N<sup>26</sup>–Fe–N<sup>171</sup> 89, 90 (94); **N<sup>26</sup>–Fe–O<sup>167</sup> 86, 90 (111)**; OW<sup>207</sup>–Fe–N<sup>81</sup> 98, 87 (90); OW<sup>207</sup>–Fe–N<sup>171</sup> 87, 89 (88); OW<sup>207</sup>–Fe–O<sup>167</sup> 89, 91 (85); **N<sup>81</sup>–Fe–N<sup>171</sup> 148, 147 (129)**; N<sup>81</sup>–Fe–O<sup>167</sup> 108, 109, (111); **N<sup>171</sup>–Fe–O<sup>167</sup> 104, 104 (120)**; values involving the second solvent-derived ligand for chain B are Fe–OW<sup>208</sup> 2.07; OW<sup>208</sup>–Fe–O<sup>167</sup> 177; OW<sup>208</sup>–Fe–N<sup>26</sup> 88; OW<sup>208</sup>–Fe–N<sup>81</sup> 70; OW<sup>208</sup>–Fe–N<sup>171</sup> 78; OW<sup>208</sup>–Fe–OW<sup>207</sup> 92.

The altered metal geometry of Fe–MnSOD means that this species has a different resting state from either native MnSOD or FeSOD. Consistent with a geometry predisposed to accepting a sixth ligand, a second exogenous ligand, OW<sup>208</sup>, binds to the Fe site of molecule B of the dimer, making that Fe six-coordinate (Figure 2).<sup>7d</sup> This ligand, assigned as a hydroxide based on spectroscopic data,<sup>8</sup> faces the base of the substrate funnel and hydrogen-bonds with the conserved residue Tyr<sup>34</sup>, which moves relative to its position in MnSOD. The other Fe site is rigorously five-coordinate.<sup>7d</sup> It seems unlikely that crystal-packing contacts between dimers, contacts that are few in number and remote to the metal sites, could influence the coordination. We believe that the unusually intimate nature of the dimer interface in the vicinity of the metal sites, which is highly conserved among all structurally characterized Mn and FeSODs, leads to active-site coupling, via the bridging loop M(A)–His<sup>171A</sup>–Glu<sup>170B</sup>–His<sup>171B</sup>–M(B), M = Fe, Mn, linking subunit A with B.<sup>3d</sup> Active-site coupling has also been proposed for a mutant Cu,Zn–SOD in which pronounced asymmetry between the two metal sites is seen;<sup>9</sup> it appears that minor asymmetry between sites in the native enzyme may become enhanced when the natural metal is changed or mutants made. The role of active-site coupling in MnSOD is currently unknown, although communication of the redox or ligand-binding state of the metal centers and redox rescue of Mn(IV) at one site in the dimer by Mn(II) have been postulated.<sup>3d</sup>

(8) (a) Whittaker, M. M.; Whittaker, J. W. *Biochemistry* **1997**, *35*, 8923–8931. (b) Yamakura, F.; Kobayashi, K.; Ue, H.; Konno, M. *Eur. J. Biochem.* **1995**, *227*, 700–706. (c) Bull, C. A.; Niederhoffer, E. C.; Yoshida, T.; Fee, J. A. *J. Am. Chem. Soc.* **1991**, *113*, 4069–4076.

(9) Hart, P. J.; Liu, Hongbin; Pellegrini, M.; Nersissian, A. M.; Gralla, E. B.; Valentine, J. S.; Eisenberg, D. *Protein Sci.* **1998**, *7*, 545–555.

The geometry of the six-coordinate hydroxide adduct of Fe–MnSOD closely resembles that found in adducts of native Mn and FeSOD with azide,<sup>2c</sup> a potent inhibitor of superoxide dismutase activity and model for hydroperoxide binding.<sup>8</sup> Azide binds to Fe–MnSOD more strongly than to FeSOD or MnSOD (with  $K_D$ 's in the relative ratio 1:5:20 under the same conditions), correlating with an increased rate of peroxide inactivation for Fe–MnSOD.<sup>8a</sup> The low catalytic activity of Fe–MnSOD in the neutral pH range may be attributed in part to the formation of a six-coordinate hydroxide adduct,<sup>8a,b</sup> which blocks substrate access to the metal center, a kinetic factor controlling activity. This is precisely what is seen in the crystal structure (in chain B). In contrast, in both native FeSOD and MnSOD, the corresponding hydrolysis,<sup>8,10</sup> and loss of catalytic activity,<sup>8</sup> occur at high pH (>10). The increased affinity of Fe–MnSOD for anions such as azide and hydroxide is evidence for a geometry that favors stabilization of six-coordinate adducts, leading to loss of functionality under conditions where native MnSOD is active. In addition, a hydrogen bond between Tyr<sup>34</sup>–OH and the “extra” hydroxide in molecule B suggest a subtle role for Tyr<sup>34</sup> in orienting and stabilizing metal-superoxide interactions. In support, mutation of Tyr<sup>34</sup> to Phe not only reduces azide and hydroxide affinity in both MnSOD and Fe–MnSOD but also decreases activity.<sup>8a</sup> These spectroscopic and X-ray data provide the structural basis to the observation that the redox potential of Fe in Fe–MnSOD (but not in FeSOD) lies below that required to oxidize superoxide ion—a crucial thermodynamic factor in controlling activity.<sup>11</sup>

These results (i) provide crystallographic evidence of enhanced anion affinity in Fe–MnSOD and verification that a second solvent-derived exogenous ligand, hydroxide, can bind to Fe–MnSOD at near-neutral pH, (ii) reveal a possible coupling between remote active sites in the dimeric protein, and (iii) provide structural evidence for altered geometry when the “wrong” metal, Fe, is substituted in MnSOD, leading to disruption of the catalytic cycle and inactivity of Fe–MnSOD under conditions where MnSOD is most active. The next challenge is to identify the structural elements or electrostatic factors<sup>12</sup> remote to the active site that lead to the altered metal geometry when the “wrong” metal is substituted in MnSOD.

**Acknowledgment.** Support from the Howard Hughes Medical Institute through the award of an International Research Scholarship (to E.N.B.) and from the United States National Institutes of Health (Grant GM42680 to J.W.W.) is gratefully acknowledged. Dedicated to Warren Roper on the occasion of his 60th birthday.

**Supporting Information Available:** Table of atomic coordinates for atoms in the vicinity of the iron sites for Fe–MnSOD and annealed omit maps in the vicinity of the iron (3 pages, print/PDF). The full set of parameters has been deposited with the Protein Data Bank (code number 1MMM). See any current masthead page for ordering information and Web access instructions.

JA981072H

(10) Tierney, D. L.; Fee, J. A.; Ludwig, M. L.; Penner-Hahn, J. E. *Biochemistry* **1995**, *34*, 1661–1668.

(11) Vance, C. K.; Miller, A.-F. *J. Am. Chem. Soc.* **1998**, *120*, 462–467.

(12) For example, the surface charge of the dimer groove between the two monomers and which passes over the metal sites is positively charged in MnSOD but negatively charged in FeSOD.<sup>3d</sup>